

Supplementary Information

Nano-Molar Level Fluorogenic and Oxidation-State Selective Chromogenic Dual Reversible Chemosensor for Multiple Targets $\text{Cu}^{2+}/\text{S}^{2-}$ and $\text{Fe}^{3+}/\text{F}^-$ ion

Sayed Muktar Hossain, Gaurab Kumar Dam, Sagarika Mishra and Akhilesh Kumar Singh*

School of Basic Sciences, Indian Institute of Technology Bhubaneswar, Bhubaneswar, 752050, India. E-mail: aksingh@iitbbs.ac.in

Contents:

Fig. S1 ESI-MS of L in methanol.
Fig. S2 ^1H NMR (400 MHz) of L in DMSO-d_6 .
Fig. S3 ^{13}C NMR (100 MHz) of L in DMSO-d_6 .
Fig. S4 FT-IR spectra of L in KBr pellet.
Fig. S5 ESI-MS of $\text{Cu}^{\text{II}}\text{L}_2$ complex in MeOH.
Fig. S6 FT-IR spectra of $\text{Cu}^{\text{II}}\text{L}_2$ complex in KBr pellet.
Fig. S7 ESI-MS of $\text{Fe}^{\text{III}}\text{L}_2$ complex in MeOH.
Fig. S8 FT-IR spectra of $\text{Fe}^{\text{III}}\text{L}_2$ complex in KBr pellet.
Table S1 Bond lengths [\AA] and angles [$^\circ$] for CuL_2 Complex $[\text{CuL}_2](\text{ClO}_4)_2$.
Fig. S9 UV-Vis spectra of L, $\text{Cu}^{\text{II}}\text{L}_2$ and $\text{Fe}^{\text{III}}\text{L}_2$ complex (20 μM each individually) in DMSO solvent.
Fig. S10 Intra-molecular non-covalent interactions ($\text{C-H}\cdots\pi$ and $\pi\cdots\pi$) present in $\text{Cu}^{\text{II}}\text{L}_2$ complex.
Fig. S11 Inter-molecular non-covalent interactions ($\text{C-H}\cdots\pi$ and $\pi\cdots\pi$) present in $\text{Cu}^{\text{II}}\text{L}_2$ complex.
Fig. S12 Job's plot for the binding of L with Fe^{3+} absorption intensity at 340 nm in MeOH was plotted as a function of the molar ratio $[\text{Fe}^{3+}] / ([\text{L}] + [\text{Fe}^{3+}])$.
Fig. S13 Detection limit of L for the recognition of Cu^{2+} ($\lambda_{\text{ex}} = 340 \text{ nm}$ and $\lambda_{\text{em}} = 407 \text{ nm}$).

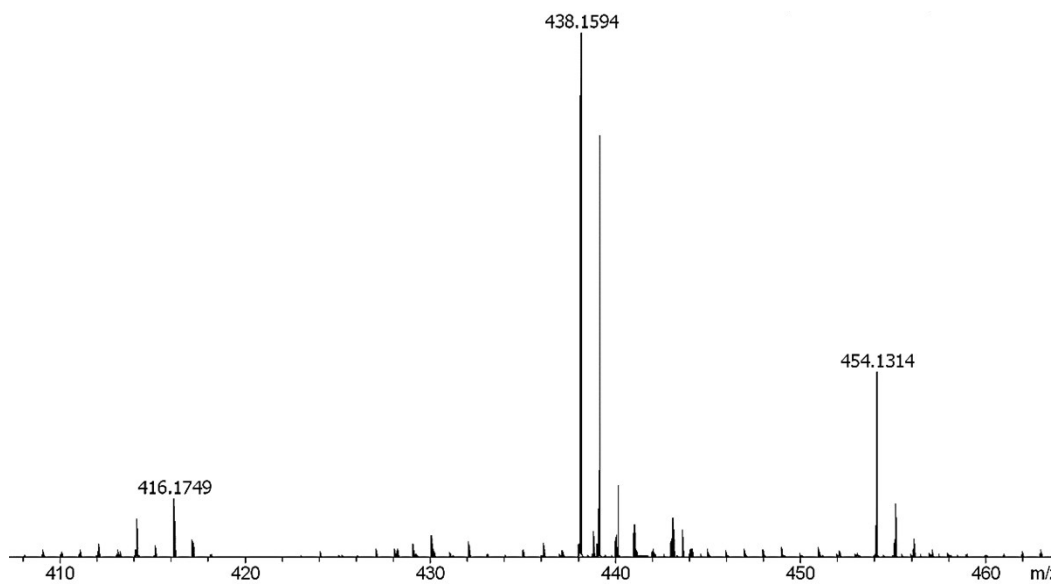


Fig. S1 ESI-MS of L in methanol.

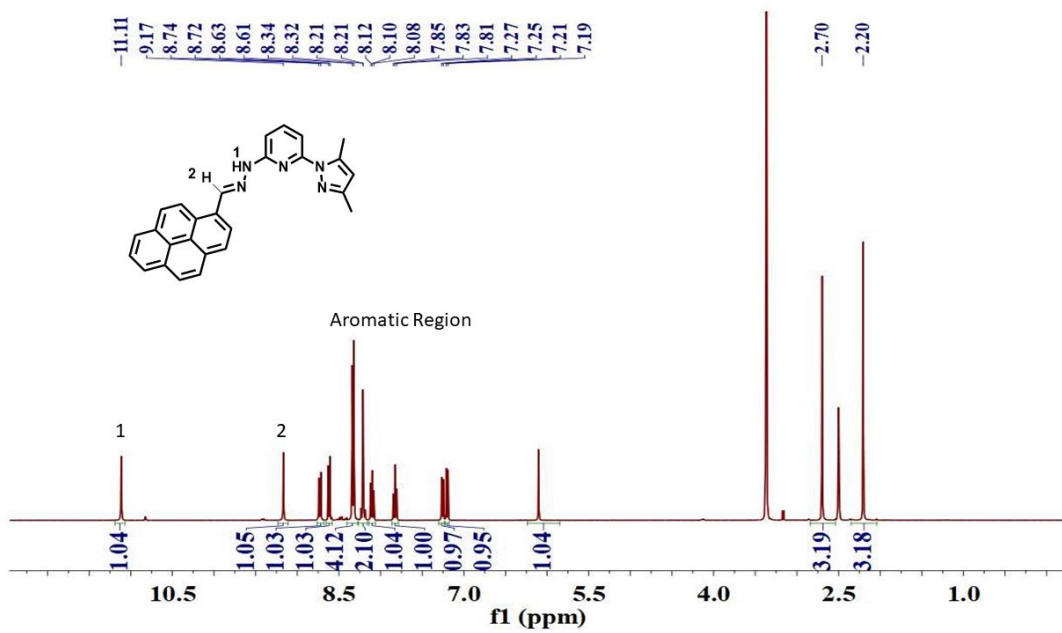


Fig. S2 ¹H NMR (400 MHz) of L in DMSO-d₆.

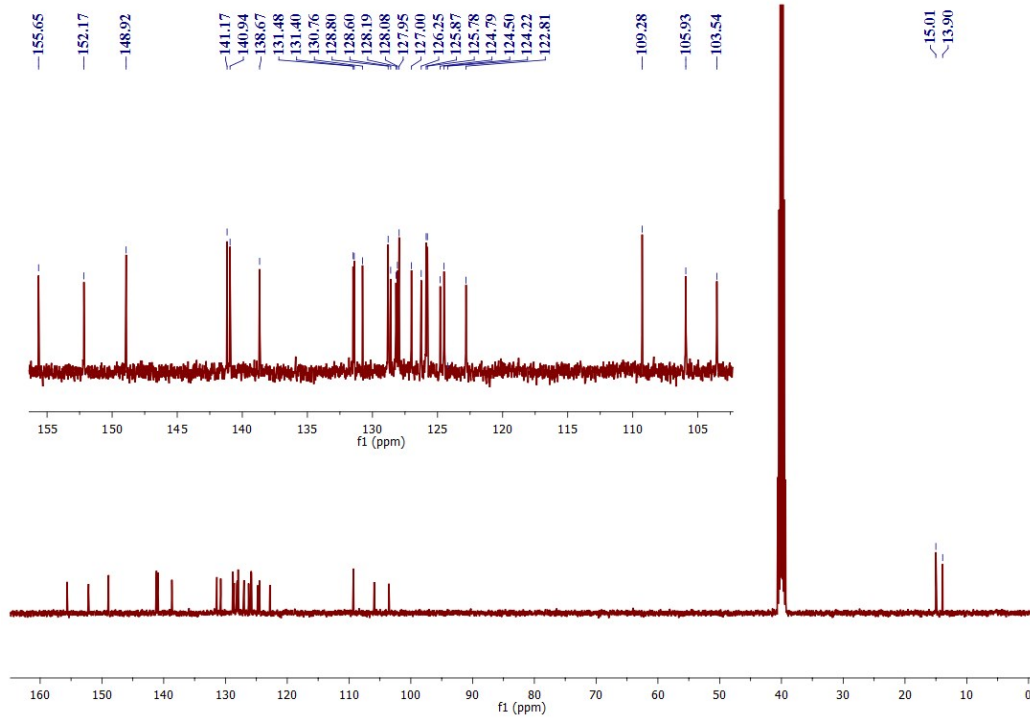


Fig. S3 ^{13}C NMR (100 MHz) of L in DMSO-d_6 .

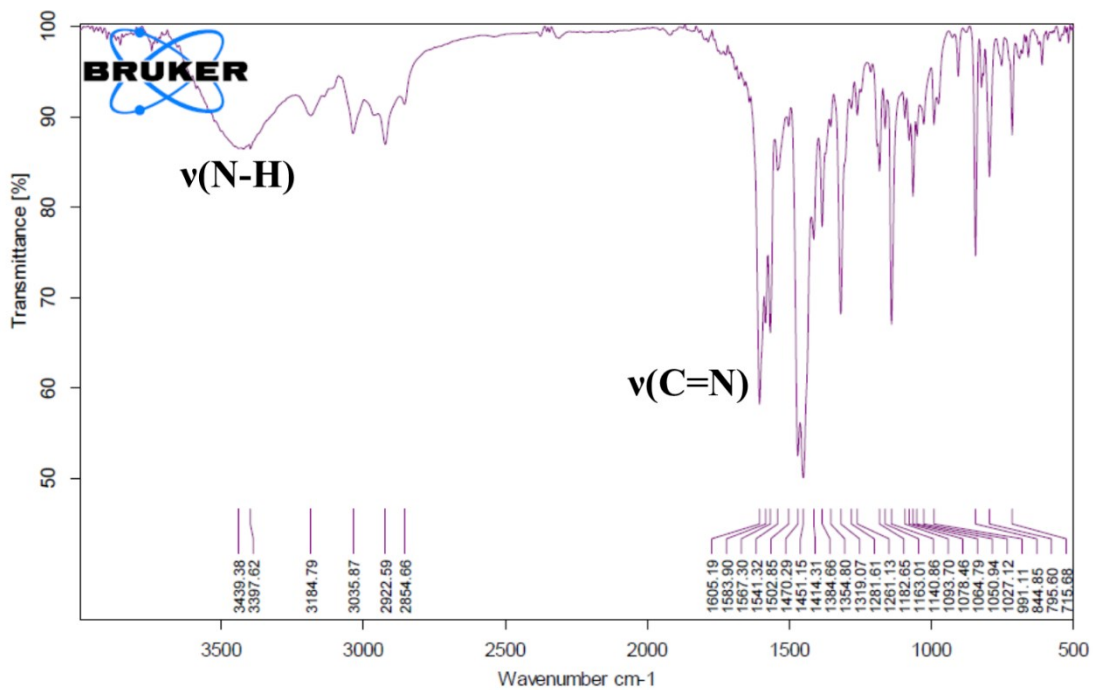


Fig. S4 FT-IR spectra of L in KBr pellet.

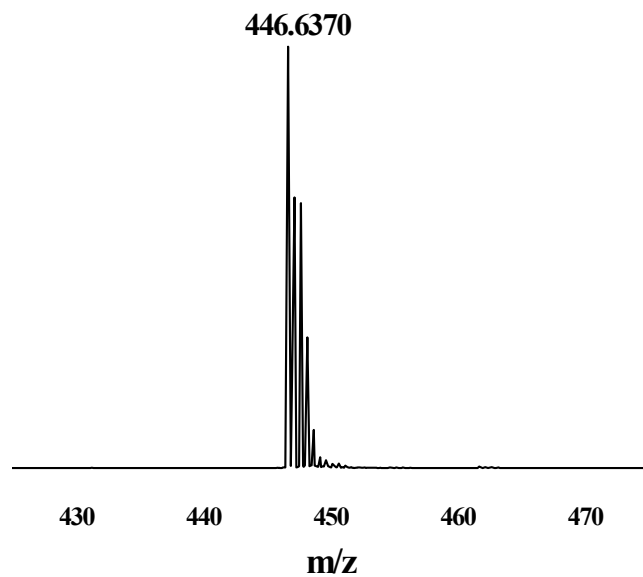


Fig. S5 ESI-MS of $\text{Cu}^{\text{II}}\text{L}_2$ complex in MeOH.

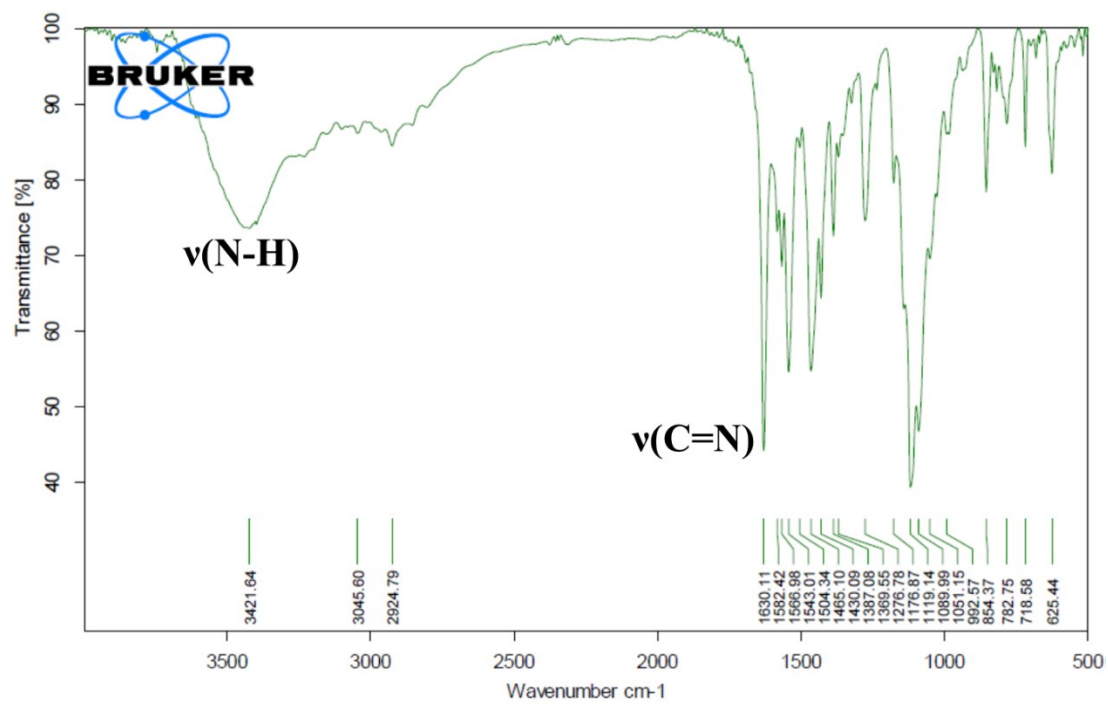


Fig. S6 FT-IR spectra of $\text{Cu}^{\text{II}}\text{L}_2$ complex in KBr pellet.

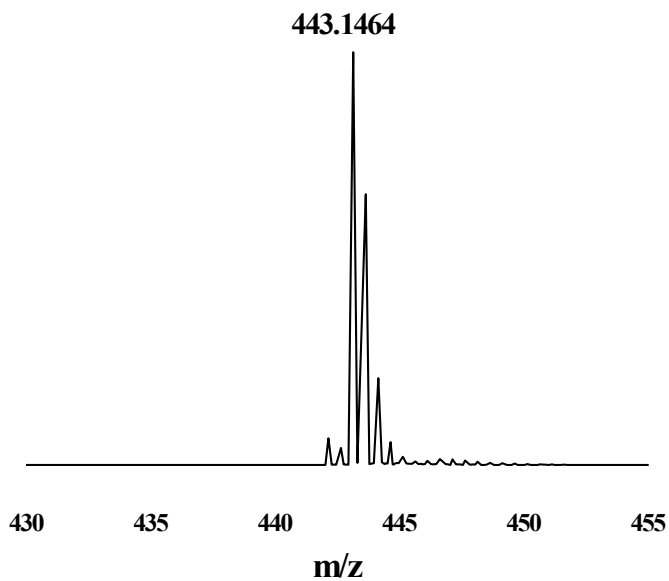


Fig. S7 ESI-MS of $\text{Fe}^{\text{III}}\text{L}_2$ complex in MeOH.

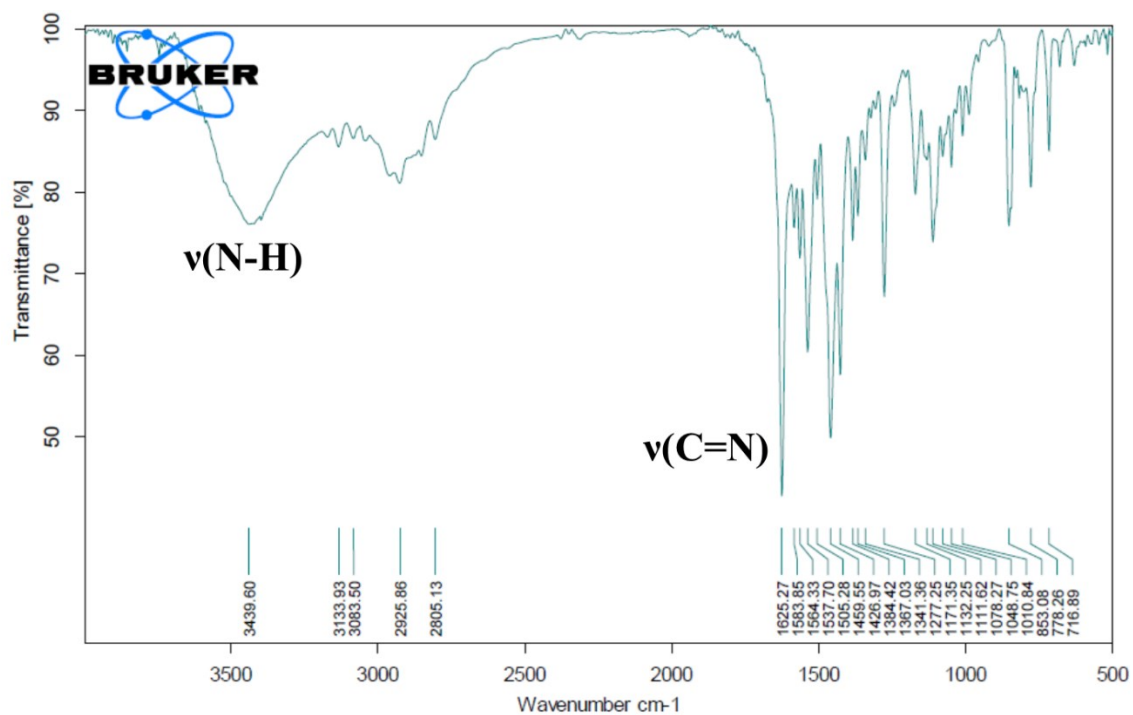


Fig. S8 FT-IR spectra of $\text{Fe}^{\text{III}}\text{L}_2$ complex in KBr pellet.

Table S1 Bond lengths [\AA] and angles [$^\circ$] for CuL_2 Complex $[\text{CuL}_2](\text{ClO}_4)_2$.

Cu(1)-N(8)	1.9511(18)
Cu(1)-N(3)	1.9660(17)
Cu(1)-N(6)	2.1147(18)
Cu(1)-N(1)	2.157(2)
Cu(1)-N(10)	2.258(2)
Cu(1)-N(5)	2.3022(19)
N(8)-Cu(1)-N(3)	179.30(8)
N(8)-Cu(1)-N(6)	78.10(7)
N(3)-Cu(1)-N(6)	101.43(7)
N(8)-Cu(1)-N(1)	103.32(8)
N(3)-Cu(1)-N(1)	77.28(7)
N(6)-Cu(1)-N(1)	102.92(8)
N(8)-Cu(1)-N(10)	76.18(7)
N(3)-Cu(1)-N(10)	104.23(7)
N(6)-Cu(1)-N(10)	153.77(7)
N(1)-Cu(1)-N(10)	88.00(8)
N(8)-Cu(1)-N(5)	103.31(7)
N(3)-Cu(1)-N(5)	76.12(7)
N(6)-Cu(1)-N(5)	86.47(7)
N(1)-Cu(1)-N(5)	153.06(7)
N(10)-Cu(1)-N(5)	94.46(8)

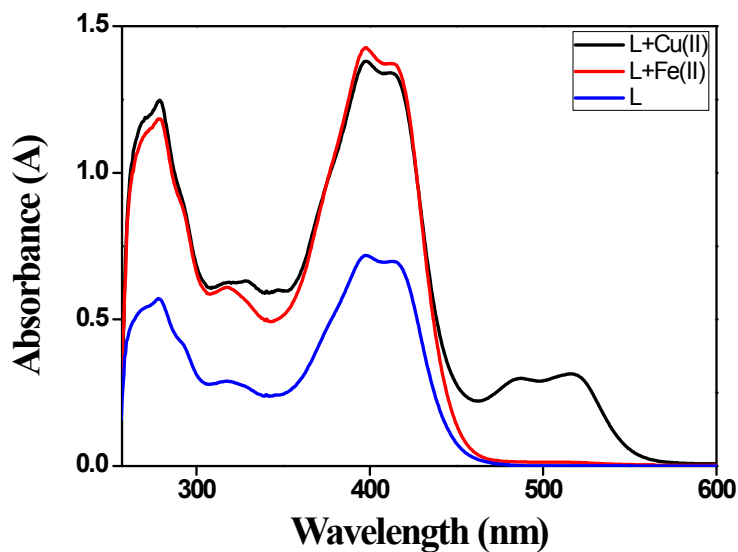


Fig. S9 UV-Vis spectra of L, $\text{Cu}^{\text{II}}\text{L}_2$ and $\text{Fe}^{\text{III}}\text{L}_2$ complex ($20 \mu\text{M}$ each individually) in DMSO solvent.

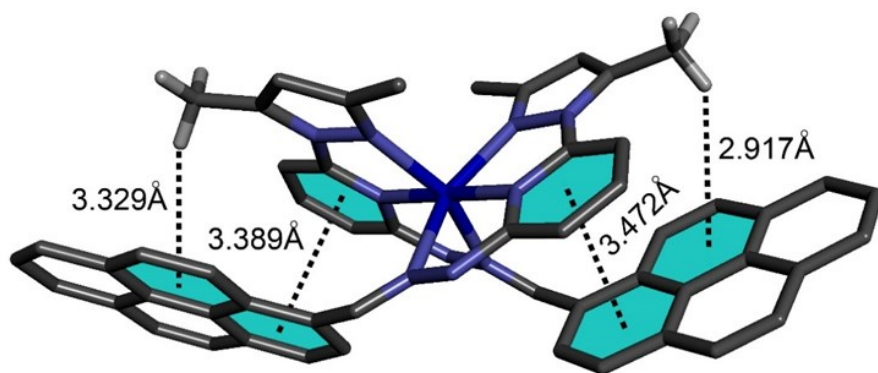


Fig. S10 Intra-molecular non-covalent interactions (C-H... π and π ... π) present in Cu^{II}L₂ complex.

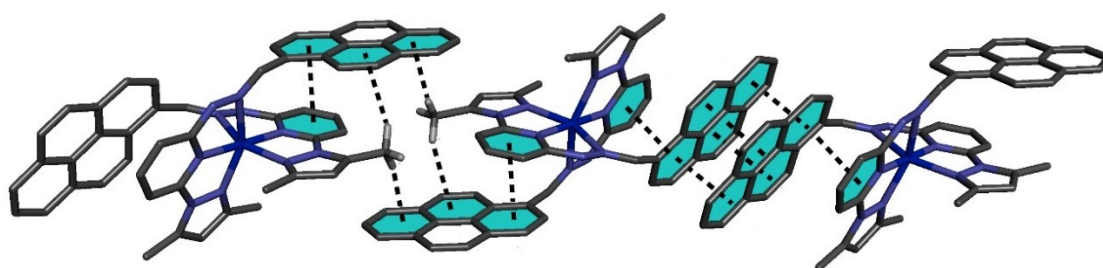


Fig. S11 Inter-molecular non-covalent interactions (C-H... π and π ... π) present in Cu^{II}L₂ complex.

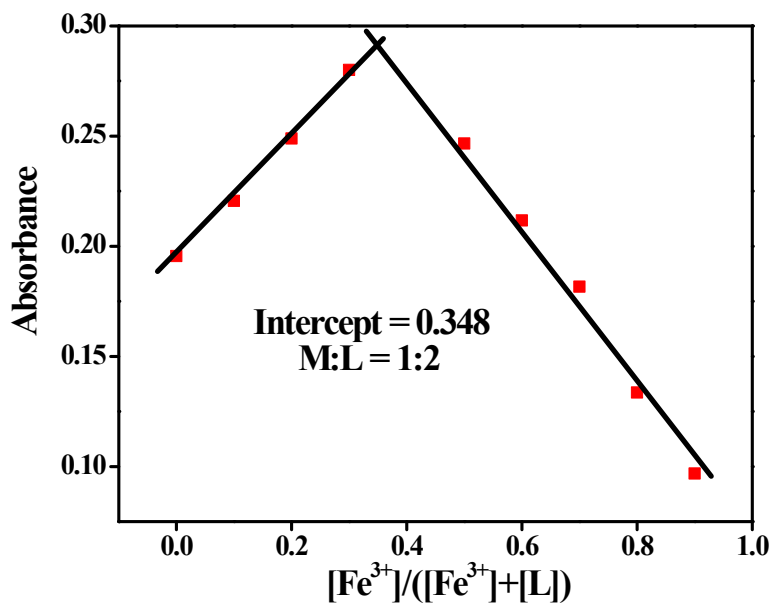


Fig. S12 Job's plot for the binding of L with Fe³⁺ absorption intensity at 340 nm in MeOH was plotted as a function of the molar ratio $[\text{Fe}^{3+}] / ([\text{L}] + [\text{Fe}^{3+}])$.

Detection limit. The detection limit was calculated on the basis of the fluorescence titration. The fluorescence emission intensity of **L** was plotted as a function of concentration of Cu^{2+} at 407 nm and the slope and intercept of plot was calculated. Then the detection limit was calculated with the following equation which was found to be very-very low 73 nM (Fig. S13).

$$\text{Detection limit} = 10^{-\left[\frac{\text{slope}}{\text{intercept}}\right]} \quad \text{eqn (2)}$$

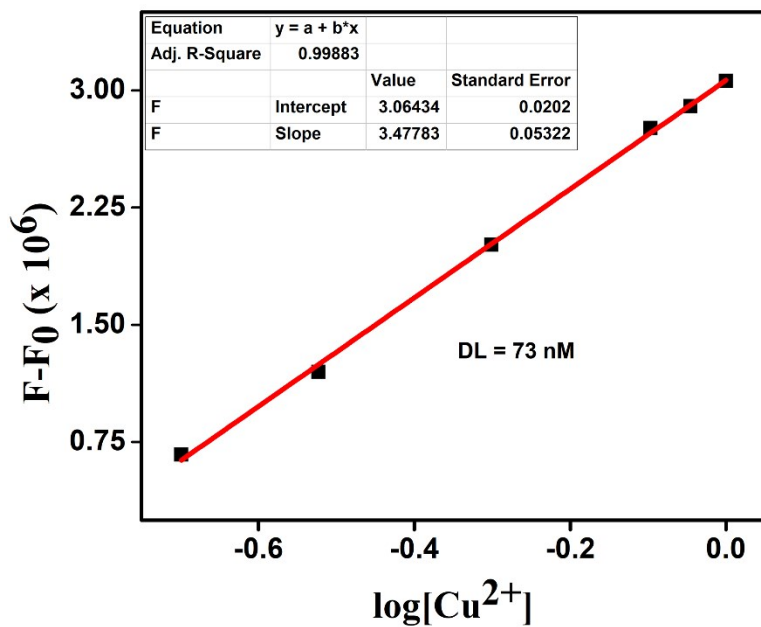


Fig. S13 Detection limit of **L** for the recognition of Cu^{2+} ($\lambda_{\text{ex}} = 340 \text{ nm}$ and $\lambda_{\text{em}} = 407 \text{ nm}$).